

PHLEGETHON, A NEARBY 60°-LONG RETROGRADE STELLAR STREAM

RODRIGO A. IBATA¹, KHYATI MALHAN¹, NICOLAS F. MARTIN^{1,2}, AND ELSE STARKENBURG³
Draft version May 11, 2022

ABSTRACT

We report the discovery of a 60° long stellar stream in Gaia DR2 catalog, found using the new **STREAMFINDER** algorithm. The structure, which is probably the remnant of a now fully disrupted globular cluster, lies ≈ 3.6 kpc away from the Sun in the direction of the Galactic bulge, and possesses highly retrograde motion. We find that the system orbits close to the Galactic plane at Galactocentric distances between 4.8 and 15.4 kpc. The discovery of this extended and extremely low surface brightness stream ($\Sigma_G \sim 34.6$ mag arcsec $^{-2}$) with a mass of only $1180 \pm 90 M_\odot$, demonstrates the power of the **STREAMFINDER** algorithm to detect even very nearby and ultra-faint structures. Due to its proximity and length we expect that Phlegethon will be a very useful probe of the Galactic acceleration field.

Keywords: Galaxy: halo — Galaxy: stellar content — surveys — galaxies: formation — Galaxy: structure

1. INTRODUCTION

The arrival of the second data release (DR2) of the Gaia mission has opened up the field of Galactic Archeology to exciting new endeavors that were previously completely out of reach. The excellent parallax and proper motion measurements (Gaia Collaboration et al. 2018d) of over a billion stars now allow the the dynamics of the various constituents of our Galaxy to be studied in great detail (Gaia Collaboration et al. 2018c,b), enabling progress towards the ultimate goal of understanding the formation of our Galaxy, its stellar components and the dark matter.

Among the Galactic components, stellar streams account for only a very minor fraction of the total mass budget, yet their astrophysical interest far exceeds their small contribution to our Galaxy. This importance stems partly from the fact that they represent fossil remnants of the accretion events that built up the Milky Way, giving us a means to ascertain the number and provenance of the building blocks of the Galactic halo (Johnston et al. 2008). Streams also roughly delineate orbits in the Galaxy, allowing one to probe the gradient of the gravitational potential (Ibata et al. 2001; Law & Majewski 2010; Varghese et al. 2011; Küpper et al. 2015) in a way that is independent of methods that make the often-unjustified assumption of dynamical equilibrium of a tracer population. Furthermore, the low velocity dispersion and fine transverse width of low-mass streams renders them excellent probes of the small-scale substructure of the dark matter halo (Ibata et al. 2002; Johnston et al. 2002; Carlberg 2012; Erkal et al. 2016).

In a previous contribution, we introduced a new algorithm (the **STREAMFINDER**; Malhan & Ibata 2018, hereafter paper I) built specifically to search efficiently through astrometric and photometric databases for

stream-like structures. The first results of this algorithm applied to Gaia DR2 were presented in Malhan et al. (2018, hereafter paper II), but were limited to distances > 5 kpc, a choice that we made in order to reduce the necessary calculation time. Here we describe a discovery based upon re-running the algorithm searching for stellar streams at distances between 0.5 and 5 kpc.

The layout of this article is as follows. Section 2 explains the selection criteria that were applied to the data and briefly summarizes the detection algorithm and adopted parameters. The results of the analysis are reported in Section 3. We present a refined fit to the stream in Section 4, and our discussion and conclusions in Section 5.

2. DATA AND STREAM ANALYSIS

All the data used in the present analysis were drawn from the Gaia DR2 catalog (Gaia Collaboration et al. 2016, 2018a). As described in paper II, we extinction-corrected the survey using the Schlegel et al. (1998) dust maps, and kept only those stars with $G_0 < 19.5$; this limiting magnitude ensures a homogeneous depth over the sky, given the additional selection criterion of choosing to analyze the sky at $|b| > 30^\circ$.

The **STREAMFINDER** works by examining every star in the survey in turn, sampling the possible orbits consistent with the observed photometry and kinematics, and finding the most likely stream fraction given a contamination model and a stream model. The adopted contamination model is identical to that built for paper II. It is an empirical model in sky position, color-magnitude and proper motion space (i.e. six-dimensions) constructed by spatially randomizing the Gaia counts with a 2° Gaussian. While the correlations between sky position and color-magnitude are recorded as binned arrays, the color-magnitude and proper motion information is condensed by the use of a 100-component Gaussian mixture model in each spatial bin.

The adopted stream model is very simple: we integrate along the sampled orbits for a half-length of 10° (i.e. total length 20°), and over this length the stream counts have uniform probability. Perpendicular to the

¹ Observatoire Astronomique, Université de Strasbourg, CNRS, 11, rue de l’Université, F-67000 Strasbourg, France; rodrigo.ibata@astro.unistra.fr

² Max-Planck-Institut für Astronomie, Königstuhl 17, D-69117 Heidelberg, Germany

³ Leibniz Institute for Astrophysics Potsdam (AIP), An der Sternwarte 16, D-14482 Potsdam, Germany

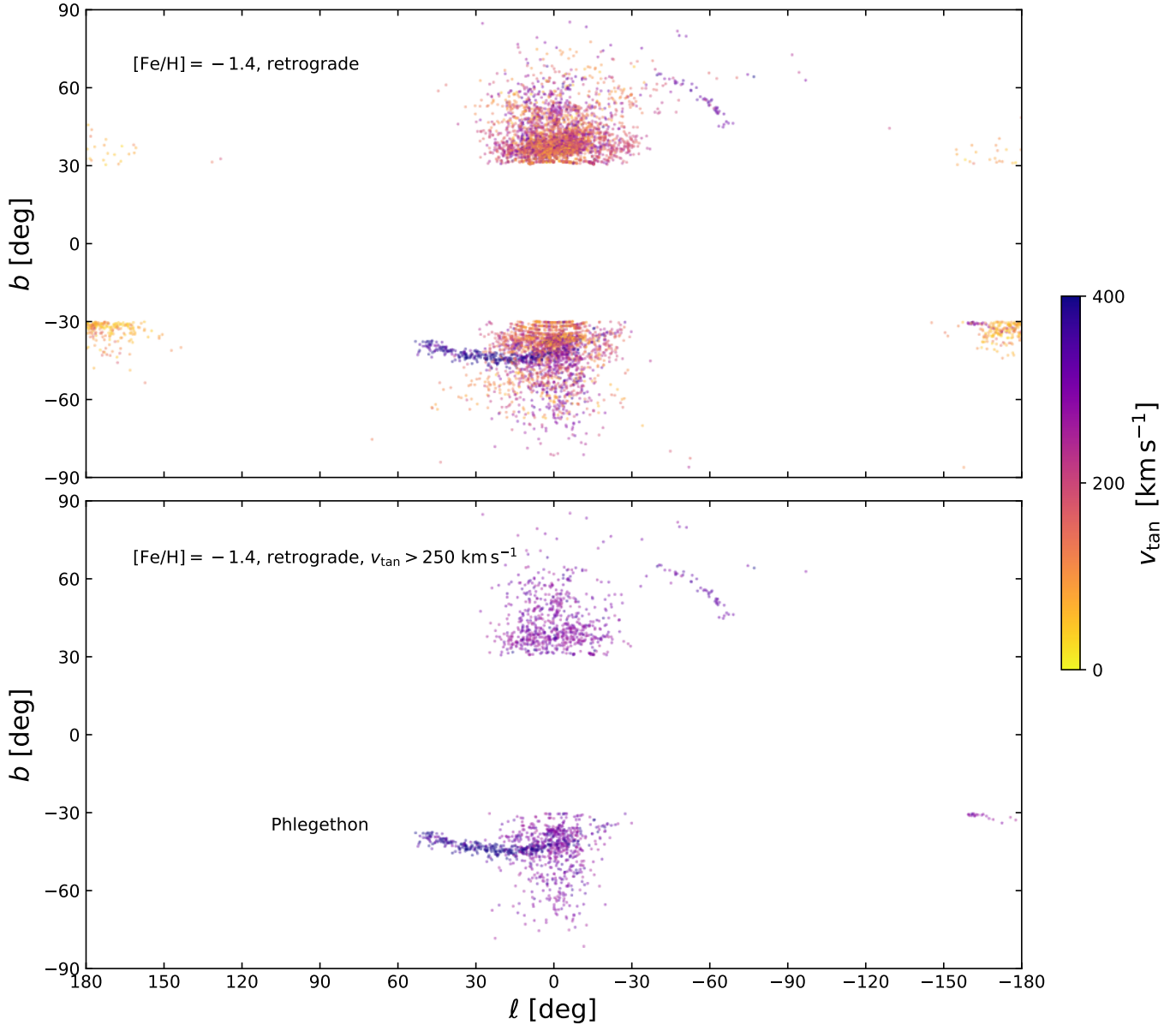


Figure 1. Output of the **STREAMFINDER** software in the distance range $[0.5, 5.0]$ kpc, assuming a stellar population of age 10 Gyr and $[\text{Fe}/\text{H}] = -1.4$. Only those stars are plotted that have retrograde orbital solutions, that lie at $|b| > 30^\circ$, and for which the stream detection significance is greater than 5σ . The upper panel shows the full range of tangential motions, while the bottom panel retains only those stars with $v_{\tan} > 250 \text{ km s}^{-1}$. Two clear streams are detected as continuous linear structures in the panels; the feature marked “Phlegethon” is the subject of the present contribution. The color of the points marks the tangential velocity of the stars, calculated using the observed Gaia proper motion in conjunction with the distance solutions that the algorithm derives for every processed star.

stream model, the properties of all observables are taken to be Gaussian, so the model has a Gaussian physical width (selected here to be 100 pc), a Gaussian dispersion in both proper motion directions equivalent to 3 km s^{-1} , and a dispersion in distance modulus of 0.05 mag. These width and velocity dispersion parameters are similar to the properties of known globular cluster streams such as the Palomar 5 stream (Dehnen et al. 2004; Ibata et al. 2016), while the distance modulus dispersion was adopted to allow for a small mismatch between the color-magnitude behavior of the adopted stellar populations model and that of the real stellar population.

The **STREAMFINDER** requires a model of the Galactic

potential in order to calculate orbits; for this we use the realistic Milky Way mass model of Dehnen & Binney (1998), their model ‘1’. The algorithm returns the best-fit orbit out of the sampled set for a given data point, the number of stars in the corresponding putative stream and the likelihood value relative to the model where the stream fraction is zero. All stars shown below have likelihoods equivalent to a stream detection exceeding the 5σ level.

To convert the kinematics of the integrated orbits into the space of observables, we assume that the Sun lies 8.20 kpc from the Galactic center and 17 pc above the Galactic mid-plane (Karim & Mamajek 2017), that

the local circular velocity is $V_{\text{circ}} = 240 \text{ km s}^{-1}$ and that the peculiar velocity of the Sun is $(u_{\odot}, v_{\odot}, w_{\odot}) = (9.0, 15.2, 7.0) \text{ km s}^{-1}$ (Reid et al. 2014; Schönrich et al. 2010).

The main aim in developing the **STREAMFINDER** was to try to find distant halo streams for which the Gaia parallax measurements are poor. To circumvent this deficiency, we use stellar populations models to convert the measured photometry into trial line of sight distance values. To this end we adopted the PARSEC isochrone models Bressan et al. (2012), covering a range in age and metallicity. Here, however, we report results using a single model with age 10 Gyr and metallicity of $[\text{Fe}/\text{H}] = -1.4$.

The stream solutions found by the **STREAMFINDER** automatically include the best-fit orbit over the trial stream length, from which one can naturally obtain an estimate of the sense of rotation of the survey stars with respect to the Galaxy. This is possible because the algorithm finds a value for the missing line of sight velocity information of a star in the Gaia DR2 catalog by requiring continuity to nearby stream candidates. The radial velocity is sampled between \pm the escape velocity, and the value corresponding to the maximum-likelihood stream solution is retained. We showed in paper II that this works for the case of well-measured streams such as GD-1 (Grillmair & Dionatos 2006). However, some associations made by the **STREAMFINDER** will be spurious, so we decided to include an additional criterion for the probability of the sense of rotation of the streams. For this, we sampled the missing line of sight velocity of each star by drawing 1000 times from a Gaussian distribution of dispersion 100 km s^{-1} and with mean equal to the component of the Sun's velocity in the direction of the star. From the fraction of draws resulting in retrograde rotation, we estimate the probability $P_{\text{retrograde}}$ that the star possesses retrograde motion, effectively under the assumption that the missing line of sight velocity is typical of that of a halo star.

3. RESULTS

In Figure 1 (top panel) we show the 1825 stars in the Gaia DR2 catalog for which the **STREAMFINDER** solutions are retrograde, and that have $P_{\text{retrograde}} > 0.9$ (as well as the parameter selections discussed previously). The color of the points encodes the tangential velocity v_{\tan} of the stars, derived from the measured proper motions and the distances estimated by the algorithm. Two stream features are clearly present in this retrograde sample, which become more evident when selecting only those stars with $v_{\tan} > 250 \text{ km s}^{-1}$ (as shown in the bottom panel). The structure that we focus on in the present contribution is labeled "Phlegethon", after the stream of the Greek Underworld. This structure forms a $\sim 60^\circ$ -long arc, skirting, in projection, the southern regions of the bulge. We delay discussion of the northern stream to Section 5.

In Figure 2 we display the proper motion distribution of the subsample of 979 stars that have $|\ell| < 120^\circ$ and $b < 0^\circ$, which reveals a continuous structure with a very large gradient in proper motion. The arc-like feature is highlighted with large (circled) dots, which are colored according to Galactic longitude; the continuous variation in color demonstrates the coherence in these

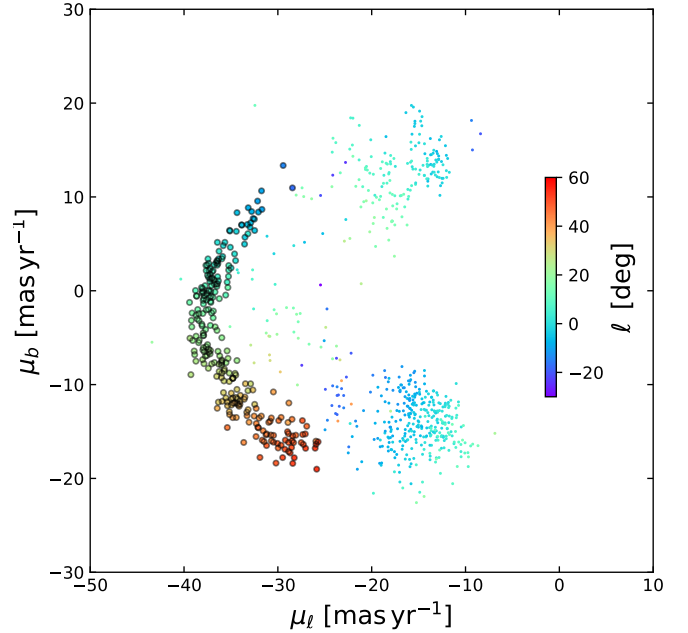


Figure 2. Proper motion distribution of the sample of stars in the lower panel of Figure 1 and that lie in the southern Galactic hemisphere. The color of the points marks Galactic longitude, which can be seen to vary continuously along the banana-shaped feature in this distribution. This distinct structure was selected to lie within an irregular hand-drawn polygon in this proper motion plane; the resulting sample are shown with the larger (black circled) dots.

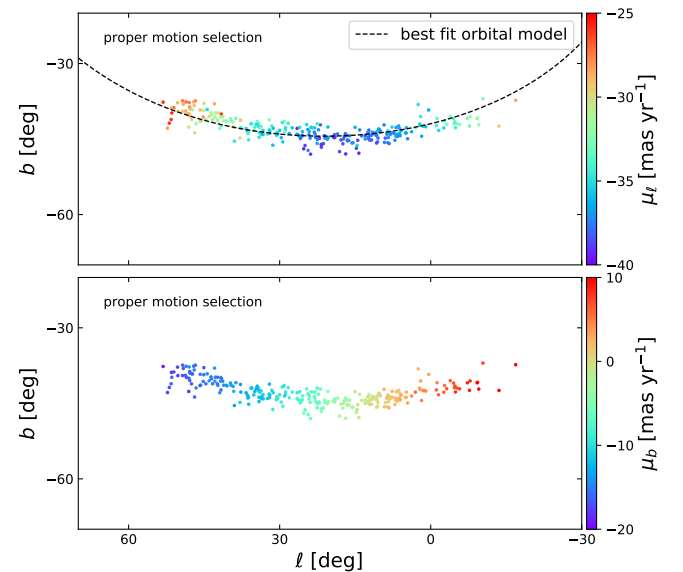


Figure 3. Sky distribution of the selection drawn from Figure 2. A very clean stream-like structure is revealed by the proper motion selection. The proper motion distribution along the stream in Galactic μ_{ℓ} and μ_b are color-coded on the top and bottom panels, respectively. The continuity of the proper motion distribution is directly obvious from the individual proper motion measurements. The dashed line in the upper panel shows the path of the best fit orbit described in Section 4.

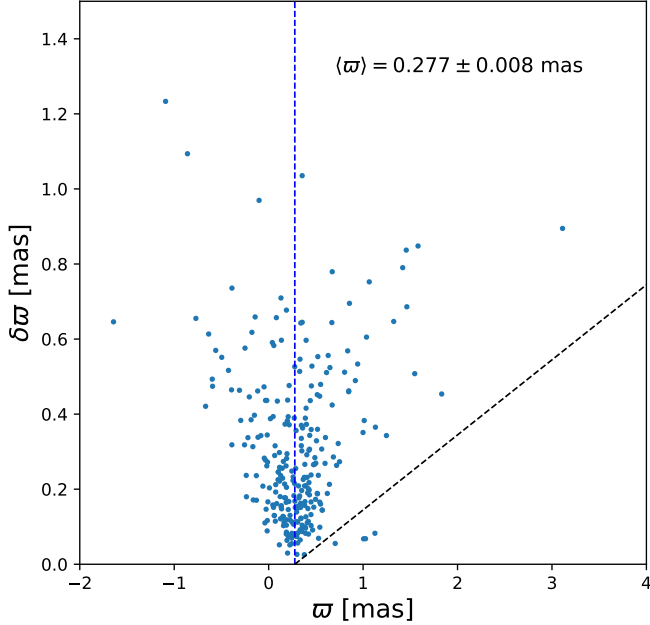


Figure 4. Parallax distribution of the stars selected in Figure 2. An iterative sigma-clipping algorithm was applied to reject the small number of parallax outliers (4 stars are discarded). The final 5σ rejection boundary is shown with the diagonal black dashed line. A maximum-likelihood fit to the remaining 264 stars gives a mean parallax of $\langle \varpi \rangle = 0.277 \pm 0.008$ mas, implying that the structure lies at a mean distance of ~ 3.6 kpc.

three parameters. These stars were selected by simply drawing an irregular polygon in the μ_ℓ , μ_b plane around this visually-obvious grouping. The distribution on the sky of the 268 sources selected in that arc are shown in Figure 3, which reveals a very clean stream-like feature. The proper motions in μ_ℓ (top panel) are strongly negative, meaning that the stars move towards the right in the Figure. Since the distance solutions provided by the algorithm predict that the structure is located at a mean heliocentric distance of 3.57 ± 0.28 kpc, the stars must be strongly lagging the Sun. Indeed, towards $\ell = 15^\circ$, the proper motion in the longitude direction reaches $\mu_\ell = -38$ mas yr $^{-1}$, implying a tangential velocity of $v_{tan} \sim 640$ km s $^{-1}$ with respect to the observer. The proper motions in the Galactic latitude direction μ_b (bottom panel) can be seen to be consistent with motion away from the plane moving rightwards from $\ell = 50^\circ$, reaching $\mu_b = 0$ at $\ell \sim 15^\circ$, and then the stars start moving towards the Galactic plane at $\ell < 15^\circ$.

If the structure is really as close as the STREAMFINDER software predicts it to be, its distance should be easily resolvable with Gaia’s parallax measurements. We display the parallaxes ϖ , along with their uncertainties $\delta\varpi$ in Figure 4. We implemented a simple maximum likelihood algorithm to calculate the mean parallax, assuming individual Gaussian parallax uncertainties on each star. This was run iteratively, starting from the STREAMFINDER distance solution, while rejecting 5σ outliers. The mean parallax was found to be $\langle \varpi \rangle = 0.277 \pm 0.008$ mas, i.e. ~ 3.6 kpc in distance, in excellent agreement with the mean distance of the STREAMFINDER solutions. Only four stars were rejected by the algorithm; they lie to the right of the diagonal dashed line in Figure 4, and they can be

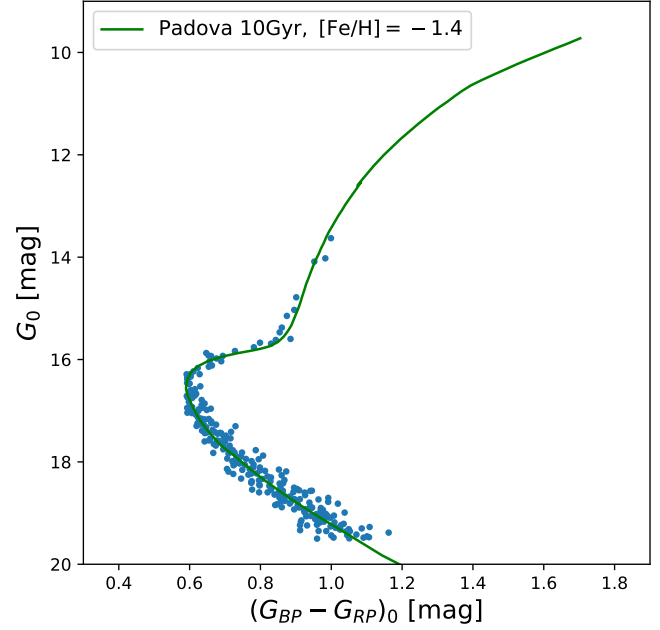


Figure 5. Color-magnitude distribution of the parallax-cleaned sample of Figure 4. The dots show the de-reddened Gaia G vs. $G_{BP} - G_{RP}$ photometry of the stars in the stream. By construction, these should follow the chosen template stellar population model (green line), but it is nevertheless a useful check to verify that the stars are not clumped in an unphysical way on the CMD. The Padova model shown here has been shifted to account for a distance modulus of 12.79 mag, as measured in Figure 4.

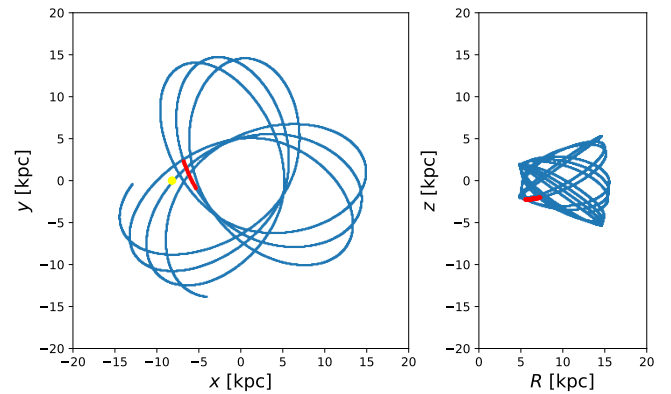


Figure 6. The orbital path of the Phlegethon stream. The MCMC procedure described in the text was used to fit the full sample simultaneously, yielding the best-fit orbit shown here. The $x - y$ plane is shown on the left panel, and the $R - z$ on the right panel, with the blue dots showing the path 1 Gyr into the past and 1 Gyr into the future. The short red region corresponds to the area where the observed stream stars are currently located. The progenitor clearly stayed close to the plane of the Galaxy on a retrograde tube orbit. In this Cartesian system, the Galactic center is at the origin, and the Sun (marked with a large yellow dot) lies at $(x, y, z) = (-8.2, 0, 0.017)$ kpc.

seen to be fairly clear outliers from the rest of the sample.

The color-magnitude distribution of the 264 stars in the final parallax-cleaned sample is displayed in Figure 5. These can be seen to conform well to the input template stellar population model, with most stars lying on the main sequence, and just a handful on the lower red giant branch. Given that the stream is approximately 60°

long and 4° wide, we deduce a system surface brightness of $\Sigma_G = 34.6 \text{ mag arcsec}^{-2}$. Adopting the template stellar population model, and accounting for the fainter (unobserved) stars, implies a mass of $1480 \pm 90 M_\odot$ over the observed region, where we have assumed that the Gaia DR2 is complete to $G_0 = 19.5$.

4. REFINED ORBITAL FITS

Although **STREAMFINDER** fits the orbits of the putative streams, it is designed for stream detection rather than careful fitting. We therefore updated the Lagrange-point stripping method described in Varghese et al. (2011), but now using the measured proper motions and parallax information as constraints. We also updated the fitting procedure to use a custom-made MCMC driver package, discussed previously in Ibata et al. (2013), that uses the affine-invariant ensemble sampling method of Goodman & Weare (2010). Since we do not know the location of the progenitor remnant, we ignored the self-gravity of the stream in the modeling, i.e. we fitted orbits over the full length of the detected structure.

The fitting parameters are sky position α, δ , distance d , heliocentric velocity v_h and proper motions μ_α, μ_δ . We chose to anchor the solutions at $\delta = -27^\circ$, approximately half-way along the stream, leaving all other parameters free to be varied by the algorithm (obviously, without an anchor line, the solution would have wandered over the full length of the stream).

After rejecting a burn-in phase of 10^5 steps, the MCMC procedure was run for a further 10^6 iterations. The best-fit orbit is shown in Figure 6, integrated over a period of 2 Gyr in the same Dehnen & Binney (1998) model employed above for stream detection. The red region marks the part of the orbit where we have currently detected the structure. The orbit is disk-like, but strongly retrograde, possessing an apocenter at $R = 15.4 \text{ kpc}$, a pericenter at 4.8 kpc and a maximum height from the Galactic plane of 5.3 kpc . As we show in Figure 7, the orbit fits the Gaia proper motions and parallax data very well, and we predict a very large heliocentric velocity gradient along the length of the stream (bottom panel). The physical length of the currently-observed portion of the stream is $\sim 3.1 \text{ kpc}$.

5. DISCUSSION AND CONCLUSIONS

In this paper, we present the discovery of a new stream structure, that we named Phlegethon, found in the recently released Gaia DR2 dataset. Phlegethon, which lies close to the Sun at a mean heliocentric distance of 3.6 kpc , possesses highly retrograde orbital motion. The rms dispersion of the stream perpendicular to the fitted orbit is 1.4° , corresponding to 88 pc at that heliocentric distance (for comparison, the Palomar 5 stream has a dispersion of 58 pc , Ibata et al. 2016). This implies that the Phlegethon stream must be the remnant of a disrupted globular cluster rather than a dwarf galaxy.

To ascertain whether Phlegethon could be related to any surviving globular cluster, in Figure 8 we compare the orbital properties (z -component of angular momentum L_z and pericenter distance) of this stream with the globular cluster sample recently analyzed by Gaia Collaboration et al. (2018b). We have labeled certain well-known retrograde globular clusters. Phlegethon clearly has extreme properties, with only NGC 3201 having a

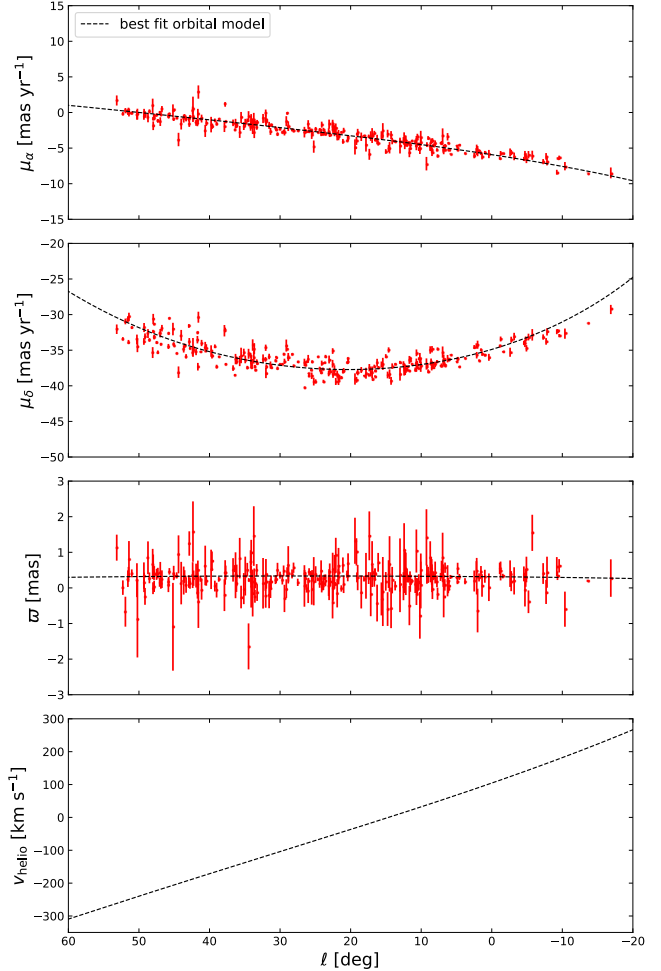


Figure 7. Comparison of the orbital solution (black dashed lines) to Gaia DR2 data (plotted in red along with their observational uncertainties). The best orbit shown previously in Figure 6 is reproduced here for a visual comparison to the data. The model captures the observed profiles in μ_α , μ_δ and ϖ , although some slight discrepancies towards the ends of the stream are apparent, possibly due to a mismatch between the real potential and the model used here. The predicted radial velocity as a function of Galactic longitude is shown on the bottom panel (this information is missing in the Gaia DR2 catalog). The orbital path in Galactic coordinates of this best-fit model was shown previously in Figure 3 (top panel).

larger value of L_z . Most importantly, however, this analysis indicates that there are no known globular clusters with similar dynamical properties to this stream, so the progenitor has probably not survived (unless by chance it is hidden in the Galactic disk).

The very low mass of $1480 \pm 90 M_\odot$ that we measure here raises an interesting puzzle. Unless the progenitor was many hundreds of times more massive than the stream segment we currently observe (which would beg the question of where the huge population of missing retrograde stars are), dynamical friction must have been completely unimportant in affecting the orbit. This would suggest that the progenitor, and later the Phlegethon stream, must have formed early in the life of the Milky Way, and continued orbiting in this disk-like but retrograde manner until the present day. It is striking then that the population appears smoothly-distributed

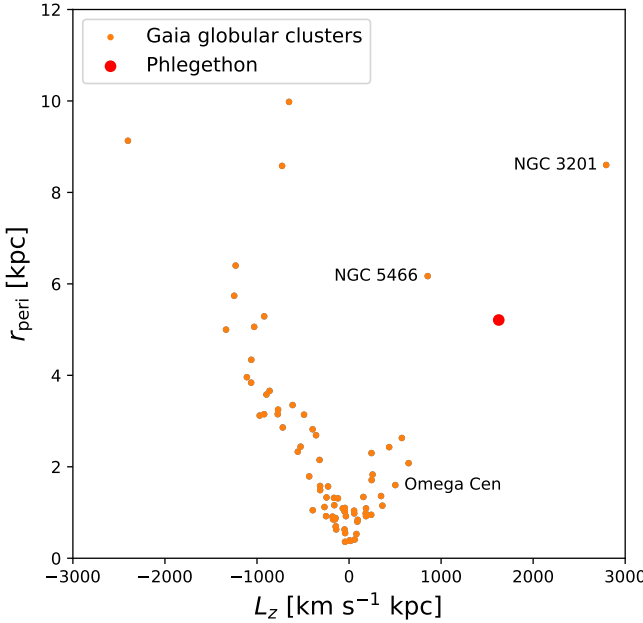


Figure 8. Orbital properties of the Phlegethon stream compared to Milky Way globular clusters. The Galactic globular clusters with orbits measured by Gaia (Gaia Collaboration et al. 2018b) are shown here in the L_z r_{peri} plane. Retrograde objects have positive L_z . The properties of Phlegethon are shown by a large red dot: it can be seen to lie far from any other globular cluster, so we conclude that the progenitor system is now completely dissolved.

on the sky (Figure 3), despite having been bombarded by dark matter sub-halos over the last 10 Gyr (the age of the stellar population as suggested by the CMD properties of the stream), and also having traversed the dense inner region of the Galactic disk every ~ 200 Myr.

It may prove very rewarding to hunt over the sky for stars with similar orbital properties. This would increase the lever-arm for orbital-fit analyses, allowing one to better test Galactic mass models. It will also allow improved constraints to be placed on the initial mass of Phlegethon’s progenitor. Interestingly, the stream seen in the northern Galactic hemisphere on the bottom panel of Figure 1 (i.e. the arc passing through $\ell = -60^\circ$, $b = 53^\circ$) has STREAMFINDER orbital solutions with L_z values that overlap those of Phlegethon; this possibility should be confirmed with radial velocity measurements of both structures.

The detection of Phlegethon shows that the STREAMFINDER algorithm can be successfully employed to find even nearby structures of exceedingly low surface brightness ($\Sigma_G \sim 34.6 \text{ mag arcsec}^{-2}$). So far, in paper II and in the present contribution we have analyzed only a small part of the parameter space of possible stream structures; our next efforts will focus on expanding the search criteria, and trying to explore further these fossil remnants in the Milky Way, examining their implications for galaxy formation and the dark matter problem.

This work has made use of data from the European Space Agency (ESA) mission *Gaia* (<https://www.cosmos.esa.int/gaia>), processed by the *Gaia* Data Processing and Analysis Consortium (DPAC, <https://www.cosmos.esa.int/web/gaia/dpac/consortium>). Funding for the DPAC has been provided by national institutions, in particular the institutions participating in the *Gaia* Multilateral Agreement.

RAI and NFM gratefully acknowledge support from a “Programme National Cosmologie et Galaxies” grant. RAI would like to thank his son Oliver for his help in naming this structure by pointing out that one of the five rivers of the Underworld was missing on previous stream maps (Grillmair 2009).

REFERENCES

Bressan, A., Marigo, P., Girardi, L., Salasnich, B., Dal Cero, C., Rubele, S., & Nanni, A. 2012, MNRAS, 427, 127

Carlberg, R. G. 2012, ApJ, 748, 20

Dehnen, W., & Binney, J. 1998, Royal Astronomical Society, 294, 429

Dehnen, W., Odenkirchen, M., Grebel, E. K., & Rix, H.-W. 2004, AJ, 127, 2753

Erkal, D., Belokurov, V., Bovy, J., & Sanders, J. L. 2016, MNRAS, 463, 102

Gaia Collaboration, Brown, A. G. A., Vallenari, A., Prusti, T., de Bruijne, J. H. J., Babusiaux, C., & Bailer-Jones, C. A. L. 2018a, arXiv, arXiv:1804.09365

Gaia Collaboration et al. 2018b, arXiv, arXiv:1804.09381

—. 2018c, arXiv, arXiv:1804.09372

—. 2018d, arXiv, arXiv:1804.09366

—. 2016, A&A, 595, A1

Goodman, J., & Weare, J. 2010, Commun. Appl. Math. Comput. Sci., 5, 65

Grillmair, C. J. 2009, ApJ, 693, 1118

Grillmair, C. J., & Dionatos, O. 2006, ApJ, 643, L17

Ibata, R., Lewis, G. F., Irwin, M., Totten, E., & Quinn, T. 2001, ApJ, 551, 294

Ibata, R., Nipoti, C., Sollima, A., Bellazzini, M., Chapman, S. C., & Dalessandro, E. 2013, MNRAS, 428, 3648

Ibata, R. A., Lewis, G. F., Irwin, M. J., & Quinn, T. 2002, MNRAS, 332, 915

Ibata, R. A., Lewis, G. F., & Martin, N. F. 2016, ApJ, 819, 1

Johnston, K. V., Bullock, J. S., Sharma, S., Font, A., Robertson, B. E., & Leitner, S. N. 2008, ApJ, 689, 936

Johnston, K. V., Spergel, D. N., & Haydn, C. 2002, ApJ, 570, 656

Karim, M. T., & Mamajek, E. E. 2017, MNRAS, 465, 472

Küpper, A. H. W., Balbinot, E., Bonaca, A., Johnston, K. V., Hogg, D. W., Kroupa, P., & Santiago, B. X. 2015, ApJ, 803, 80

Law, D. R., & Majewski, S. R. 2010, ApJ, 714, 229

Malhan, K., & Ibata, R. 2018, arXiv, 4063

Malhan, K., Ibata, R. A., & Martin, N. F. 2018, arXiv, arXiv:1804.11339

Reid, M. J., et al. 2014, ApJ, 783, 130

Schlegel, D. J., Finkbeiner, D. P., & Davis, M. 1998, ApJ, 500, 525

Schönrich, R., Binney, J., & Dehnen, W. 2010, MNRAS, 403, 1829

Varghese, A., Ibata, R., & Lewis, G. F. 2011, MNRAS, 417, 198